2009 IEEE/ASME International Conference on Advanced Intelligent Mechatronics
Suntec Convention and Exhibition Center
Singapore, July 14-17, 2009

Coordinated Contouring Controller Design for an Industrial Biaxial Linear Motor Driven Gantry

Chuxiong Hu, Bin Yao, and Qingfeng Wang

***Abstract*—To improve overall contouring performance, it is no longer possible to neglect dynamic coupling phenomena that occur during contouring operations, especially for linear motor driven systems which often move at high speeds. This paper studies the high performance contouring control of a linear motors driven high-speed/acceleration industrial biaxial gantry. The gantry dynamics is first transformed into a task coordinate frame. A discontinuous projection based adaptive robust controller (ARC) which explicitly takes into account the dynamic coupling effect is then constructed to improve the contouring performance under both parametric uncertainties and uncertain nonlinearities. To reduce the effect of measurement noise, a desired compensation ARC (DCARC) scheme is also presented, in which the adaptive model compensation part depends on the desired contour and parameter estimates only. Comparative experimental results of the proposed algorithms along with a well tuned PID controller are obtained on a high-speed industrial biaxial gantry driven by linear motors. The results verify that both the proposed schemes outperform the PID controller and can achieve good contouring performance even in the presence of parametric uncertainties and uncertain disturbances, and the desired compensation ARC achieves the best contouring performance.**

***Index Terms*—Contouring, coordinated control, linear motors, task coordinates, adaptive robust control.**

I. Introduction

As one of the most popular solutions to high-speed and high-precision motion applications, linear motors driven systems have attracted significant attentions during the past decade. A great deal of efforts have been devoted to solving independent axial control problems of these devices [1], [2], [3]. In those designs, each axis of motion is separately driven and the servo controller of each axis receives no information from other axes, which results in a collection of decoupled single input and single output (SISO) control designs. Decoupled design may be preferable if the disturbance in one axis should not affect the performance of other axes. For contouring applications, however, decoupling is sometimes damaging to the overall performance objective [4].

The work is supported in part by the US National Science Foundation (Grant No. CMS-0600516) and in part by the National Natural Science Foundation of China (NSFC) under the Joint Research Fund for Overseas Chinese Young Scholars (Grant No. 50528505).

Chuxiong Hu, a PhD student, and Qingfeng Wang, a professor, are with the State Key Laboratory of Fluid Power Transmission and Control, Zhejiang University, Hangzhou, China. Their emails are fyfox.hu@gmail.com and qfwang@zju.edu.cn

Bin Yao is a Professor of School of Mechanical Engineering at Purdue University, West Lafayette, IN 47907, USA (byao@purdue.edu). He is also a Kuang-piu Professor at the State Key Laboratory of Fluid Power Transmission and Control of Zhejiang University.

A more appropriate approach to address the contouring control problem is to introduce coupling actions in the servo controllers so that the motion axes are "coordinated" to track the desired contour. In [5], Koren first proposed the cross-coupled control (CCC) strategy dedicated to improve the coordination of axes. By simultaneously feeding the CCC signal into all the axial tracking loops, the control of one axial servomechanism was affected by other axial servomechanisms involved in the motion and consequently the coordination of axes was increased. Since then, many research publications on CCC have been reported [6], [7], [8]; for instance, Koren and Lo [6] introduced a variable-gain cross-coupled controller for a general class of contours by estimating the magnitude and the direction of contouring errors for further compensation. However, they cannot effectively address the dynamic coupling phenomena (e.g. Coriolis force) occur when tracking curved contours, since these designs are based on the traditional control theories for linear time-invariant systems.

In recent years, contouring control problems were studied by using different control methods. Chiu and Tomizuka [4] formulated the contour tracking problem in the task coordinate frame which is "attached" to the desired contour. Under the task coordinate formulation, a control law can be designed to assign different dynamics to the normal and tangential directions relative to the desired contour. Based on such a task coordinate approach, many contouring control schemes have been reported [9], [10]. For example, Chen, Lou and Li [9] developed an adaptive contouring controller in the task coordinate frame to handle bounded external disturbances and system model uncertainties while maintaining certain contouring performance. However, the principal shortcoming of these existing control techniques is that they cannot explicitly incorporate parametric uncertainties and uncertain nonlinearities in the formulation of contouring control problems. As a result, when stringent contouring performance is of major concerns, these methods may be insufficient.

In this paper, the adaptive robust control (ARC) strategy developed by Yao in [11] is utilized to solve the high-speed/accuracy contouring control problem of an industrial biaxial linear motor driven gantry. The gantry dynamics is first transformed into a task coordinate frame. A discontinuous projection based adaptive robust controller [11] is then constructed to improve the contouring performance. This algorithm may have several potential implementation limitation since the regressor used in parameter adaptation law depends on the actual measurement of system states. To overcome those limitations, the desired compensation ARC strategy in [12] is also applied to develop a coordinated ARC contouring

978-1-4244-2853-3/09/$25.00 ©2009 IEEE

controller in which the regressor is calculated based on the desired contour information only. The proposed ARC and DCARC along with a well tuned PID are all implemented on a high-speed Anorad industrial biaxial gantry driven by LC-50-200 linear motors with a linear encoder resolution of 0.5 μm. Comparative experimental results have been obtained and verified that both ARC and DCARC schemes outperform the PID controller and can achieve good contouring performance even in the presence of parametric uncertainties and uncertain disturbance. Comparative experimental results also demonstrate that the DCARC achieves the best contouring performance.

II. Problem Formulation

A. Task Coordinate Frame

Accurate calculation of contouring error often leads to an intensive computation task which is hard to be realized in practice. Therefore, for the contour tracking purposes, this definition is often replaced by approximate models [10]. A

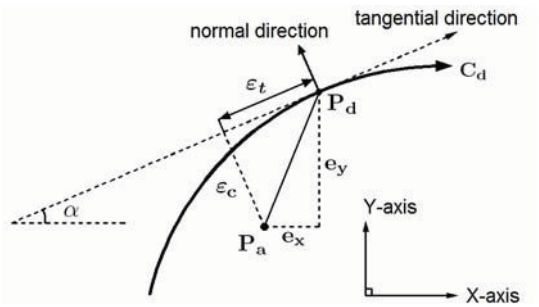

Figure 1. An Approximate Contouring Error Model

very popular estimation of contouring error is presented in [7], [10] as shown in Figure 1. Let x and y denote the horizontal and the vertical axes of a biaxial gantry system. At any time instant, there are two points P_d and P_a denoting the position of the reference command and the actual position of the system, respectively. For the point P_d, it possesses a set of tangential and normal directions such that the contouring error can be approximated by the distance from P_a to the tangential line in the normal direction. By this definition, the contouring error ε_c can be approximately computed by the normal error ε_n as:

$$\varepsilon_c \approx \varepsilon_n = -sin\alpha \cdot e_x + cos\alpha \cdot e_y \tag{1}$$

where e_x and e_y denote the axial tracking errors of x and y axes, i.e. $e_x = x - x_d$, $e_y = y - y_d$, and α denotes the angle between the tangential line to the horizontal X-axis. In this model, if the axial tracking errors are comparatively small to the curvature of the desired contour, then it yields a good approximation of the contouring error.

The tangential error ε_t in Figure 1 can be described as

$$\varepsilon_t = cos\alpha \cdot e_x + sin\alpha \cdot e_y \tag{2}$$

Then the tangential and the normal directions are mutually orthogonal and hence can be taken as the new basis for the task coordinate frame. Then the physical (x,y) coordinates can be transformed into the task $(\varepsilon_c, \varepsilon_t)$ coordinates by a linear time-varying transformation

$$\boldsymbol{\varepsilon} = \mathbf{T}\mathbf{e} \tag{3}$$

where $\boldsymbol{\varepsilon} = [\varepsilon_c, \varepsilon_t]^T$; $\mathbf{e} = [e_x, e_y]^T$, and the transformation matrix is

$$\mathbf{T} = \begin{bmatrix} -sin\alpha & cos\alpha \\ cos\alpha & sin\alpha \end{bmatrix} \tag{4}$$

The matrix T is always unitary for all values of α, i.e., $\mathbf{T^T} = \mathbf{T}$ and $\mathbf{T^{-1}} = \mathbf{T}$.

B. System Dynamics

The biaxial linear motor driven gantry is assumed to have the following dynamics:

$$\mathbf{M}\ddot{\mathbf{q}} + \mathbf{B}\mathbf{q} + \mathbf{F}(\dot{\mathbf{q}}) = \mathbf{u} + \mathbf{d}; \tag{5}$$

where $\mathbf{q} = [x(t), y(t)]^T$, $\dot{\mathbf{q}} = [\dot{x}(t), \dot{y}(t)]^T$ and $\ddot{\mathbf{q}} = [\ddot{x}(t), \ddot{y}(t)]^T$ are the 2×1 vectors of the axis position, velocity and acceleration, respectively; $\mathbf{u}$ is the 2×1 vector of control input, and $\mathbf{d}$ is the 2×1 vector of unknown nonlinear functions due to external disturbances or modeling errors such as the force ripple; $\mathbf{M} = diag[M_1, M_2]$ and $\mathbf{B} = diag[B_1, B_2]$ are the 2×2 diagonal inertia and damping matrices, respectively; $\mathbf{F}(\dot{\mathbf{q}})$ is the 2×1 vector of nonlinear friction, and the model used in this paper is given by $\bar{\mathbf{F}}(\dot{\mathbf{q}}) = \mathbf{A}\mathbf{S_f}(\dot{\mathbf{q}})$, where $\mathbf{A} = diag[A_1, A_2]$ is the 2×2 diagonal friction coefficient matrix, and $\mathbf{S_f}(\cdot)$ is a vector-valued smooth function, i.e., $\mathbf{S_f}(\dot{\mathbf{q}}) = [S_f(\dot{x}), S_f(\dot{y})]^T$. Define the approximation error as $\widetilde{\mathbf{F}} = \bar{\mathbf{F}} - \mathbf{F}$. Then equation (5) can be written as

$$\mathbf{M}\ddot{\mathbf{q}} + \mathbf{B}\dot{\mathbf{q}} + \mathbf{A}\mathbf{S_f}(\dot{\mathbf{q}}) = \mathbf{u} + \mathbf{d_n} + \widetilde{\mathbf{d}} \tag{6}$$

where $\mathbf{d_n} = [d_{n1}, d_{n2}]^T$ is the nominal value of $\mathbf{d_1} = \mathbf{d} + \widetilde{\mathbf{F}}$, and $\widetilde{\mathbf{d}} = \mathbf{d_1} - \mathbf{d_n}$. For this dynamic system, we define the tracking error as $\mathbf{e} = [e_x, e_y]^T = [x(t) - x_d(t), y(t) - y_d(t)]^T$ where $\mathbf{q_d}(t) = [x_d(t), y_d(t)]^T$ is given to describe the desired contour. Then the system dynamics can be rewritten as

$$\mathbf{M}\ddot{\mathbf{e}} + \mathbf{B}\dot{\mathbf{e}} + \mathbf{A}\mathbf{S_f}(\dot{\mathbf{q}}) + \mathbf{M}\ddot{\mathbf{q}}_\mathbf{d} + \mathbf{B}\dot{\mathbf{q}}_\mathbf{d} = \mathbf{u} + \mathbf{d_n} + \widetilde{\mathbf{d}} \tag{7}$$

Noting (3) and (4) and the unitary property of $\mathbf{T}$, the time derivatives of the tracking error states can be derived as

$$\dot{\mathbf{e}} = \mathbf{T}\dot{\boldsymbol{\varepsilon}} + \dot{\mathbf{T}}\boldsymbol{\varepsilon}, \ddot{\mathbf{e}} = \mathbf{T}\ddot{\boldsymbol{\varepsilon}} + \mathbf{2}\dot{\mathbf{T}}\dot{\boldsymbol{\varepsilon}} + \ddot{\mathbf{T}}\boldsymbol{\varepsilon} \tag{8}$$

Then the system dynamics can be represented in the task coordinate frame as

$$\begin{aligned} &\mathbf{M_t}\ddot{\boldsymbol{\varepsilon}} + \mathbf{B_t}\dot{\boldsymbol{\varepsilon}} + 2\mathbf{C_t}\dot{\boldsymbol{\varepsilon}} + \mathbf{D_t}\boldsymbol{\varepsilon} + \mathbf{M_q}\ddot{\mathbf{q}}_\mathbf{d} + \mathbf{B_q}\dot{\mathbf{q}}_\mathbf{d} + \mathbf{A_q}\mathbf{S_f}(\dot{\mathbf{q}}) \\ &= \mathbf{u_t} + \mathbf{d_t} + \widetilde{\Delta} \end{aligned} \tag{9}$$

where

$$\begin{aligned} &\mathbf{M_t} = \mathbf{TMT}, \mathbf{B_t} = \mathbf{TBT}, \mathbf{C_t} = \mathbf{TM}\dot{\mathbf{T}}, \\ &\mathbf{D_t} = \mathbf{TM}\ddot{\mathbf{T}} + \mathbf{TB}\dot{\mathbf{T}}, \mathbf{u_t} = \mathbf{Tu}, \mathbf{d_t} = \mathbf{Td_n}, \widetilde{\Delta} = \mathbf{T}\widetilde{\mathbf{d}}, \\ &\mathbf{M_q} = \mathbf{TM}, \mathbf{B_q} = \mathbf{TB}, \mathbf{A_q} = \mathbf{TA} \end{aligned} \tag{10}$$

It is well known that equation (9) has several properties:

(P1) In the finite work space $\mathbf{q} \in \Omega_\mathbf{q}$, $\mathbf{M_t}$ is a symmetric positive definite (s.p.d.) matrix with

$$\mu_1 \mathbf{I} \leq \mathbf{M_t} \leq \mu_2 \mathbf{I}, \ \forall \mathbf{q} \in \Omega_\mathbf{q}, \tag{11}$$

where μ_1 and μ_2 are two positive scalars.

(P2) The matrix $\mathbf{N} = \dot{\mathbf{M}}_\mathbf{t} - \mathbf{2C_t}$ is zero.

(P3) The task space dynamics (9) is linear in terms of a set of parameters, such as inertia $\mathbf{M}$, damping coefficient $\mathbf{B}$, friction coefficient $\mathbf{A}$ and nominal disturbance $\mathbf{d_n}$, i.e.,

$$\begin{aligned}&\mathbf{M_t}\ddot{\varepsilon} + \mathbf{B_t}\dot{\varepsilon} + \mathbf{2C_t}\dot{\varepsilon} + \mathbf{D_t}\varepsilon + \mathbf{M_q}\ddot{\mathbf{q}}_\mathbf{d} + \mathbf{B_q}\dot{\mathbf{q}}_\mathbf{d} + \mathbf{A_q}\mathbf{S_f}(\dot{\mathbf{q}}) - \mathbf{d_t} \\ &= -\varphi(\mathbf{q}, \dot{\mathbf{q}}, t)\theta\end{aligned} \tag{12}$$

where φ is a 2×8 matrix of known functions, known as the **regressor**, and θ is an 8-dimensional vector of unknown parameters defined as $\theta = [\theta_1, ..., \theta_8]^T = [M_1, M_2, B_1, B_2, A_1, A_2, d_{n1}, d_{n2}]^T$.

In general, the parameter vector θ cannot be known exactly. For example, the payload of the biaxial gantry depends on tasks. However, the extent of parametric uncertainties can be predicted. Therefore, the following practical assumption is made. (For simplicity, the following notations are used: $\bullet_i$ for the i-th component of the vector $\bullet$, $\bullet_{min}$ for the minimum value of $\bullet$, and $\bullet_{max}$ for the maximum value of $\bullet$. The operation $\leq$ for two vectors is performed in terms of the corresponding elements of the vectors.)

Assumption 1: The extent of the parametric uncertainties and uncertain nonlinearities is known, i.e.,

$$\theta \in \Omega_\theta \triangleq \{\theta : \ \theta_{min} \leq \theta \leq \theta_{max}\} \tag{13}$$

$$\widetilde{\Delta} \in \Omega_\Delta \triangleq \left\{\widetilde{\Delta} : \ ||\widetilde{\Delta}|| \leq \delta_\Delta\right\} \tag{14}$$

where $\theta_{min} = [\theta_{1min}, ..., \theta_{8min}]^T$, and $\theta_{max} = [\theta_{1max}, ..., \theta_{8max}]^T$ are known. δ_Δ is a known function.

The control objective is to synthesize a control input $\mathbf{u_t}$ such that $\mathbf{q} = [x, y]^T$ tracks a desired contour $\mathbf{q_d}(t) = [x_d, y_d]^T$ which is assumed to be at-least second-order differentiable.

III. Discontinuous Projection

Let $\widehat{\theta}$ denote the estimate of θ and $\widetilde{\theta}$ the estimation error (i.e., $\widetilde{\theta} = \widehat{\theta} - \theta$). In view of (13), the following adaptation law with discontinuous projection modification can be used

$$\dot{\widehat{\theta}} = Proj_{\widehat{\theta}}(\Gamma\tau) \tag{15}$$

where $\Gamma > 0$ is a diagonal matrix, τ is an adaptation function to be synthesized later. The projection mapping $Proj_{\widehat{\theta}}(\bullet) = [Proj_{\widehat{\theta}_1}(\bullet_1), ..., Proj_{\widehat{\theta}_8}(\bullet_8)]^T$ is defined in [11] as

$$Proj_{\widehat{\theta}_i}(\bullet_i) = \begin{cases} 0 & if\ \widehat{\theta}_i = \theta_{imax}\ and\ \bullet_i > 0 \\ 0 & if\ \widehat{\theta}_i = \theta_{imin}\ and\ \bullet_i < 0 \\ \bullet_i & otherwise \end{cases} \tag{16}$$

It can be shown that for any adaptation function τ, the projection mapping used in (16) guarantees

(P4)

$$\widehat{\theta} \in \Omega_\theta \triangleq \left\{\widehat{\theta} : \theta_{imin} \leq \widehat{\theta} \leq \theta_{imax}\right\} \tag{17}$$

(P5)

$$\widetilde{\theta}^T(\Gamma^{-1} Proj_{\widehat{\theta}}(\Gamma\tau) - \tau) \leq 0, \ \forall\tau \tag{18}$$

IV. Adaptive Robust Control (ARC) Law

Define a switching-function-like quantity as

$$\mathbf{s} = \dot{\varepsilon} + \Lambda\varepsilon \tag{19}$$

where $\Lambda > 0$ is a diagonal matrix. Define a positive semi-definite (p.s.d.) function

$$V(t) = \tfrac{1}{2}\mathbf{s^T M_t s} \tag{20}$$

Differentiating V yields

$$\begin{aligned}\dot{V} = \mathbf{s^T}[&\mathbf{u_t} + \mathbf{d_t} + \widetilde{\Delta} - \mathbf{M_q}\ddot{\mathbf{q}}_\mathbf{d} - \mathbf{B_q}\dot{\mathbf{q}}_\mathbf{d} - \mathbf{A_q}\mathbf{S_f}(\dot{\mathbf{q}}) \\ &- \mathbf{B_t}\dot{\varepsilon} - \mathbf{C_t}\dot{\varepsilon} - \mathbf{D_t}\varepsilon + \mathbf{C_t}\Lambda\varepsilon + \mathbf{M_t}\Lambda\dot{\varepsilon}]\end{aligned} \tag{21}$$

where (P2) is used to eliminate the term $\frac{1}{2}\mathbf{s^T}\dot{\mathbf{M}}_\mathbf{t}\mathbf{s}$. Furthermore, following (P3), similarly we can define

$$\begin{aligned}&\mathbf{M_q}\ddot{\mathbf{q}}_\mathbf{d} + \mathbf{B_q}\dot{\mathbf{q}}_\mathbf{d} + \mathbf{A_q}\mathbf{S_f}(\dot{\mathbf{q}}) + \mathbf{B_t}\dot{\varepsilon} + \mathbf{C_t}\dot{\varepsilon} + \mathbf{D_t}\varepsilon \\ &- \mathbf{C_t}\Lambda\varepsilon - \mathbf{M_t}\Lambda\dot{\varepsilon} - \mathbf{d_t} = -\Psi(\mathbf{q}, \dot{\mathbf{q}}, t)\theta\end{aligned} \tag{22}$$

where Ψ is a 2×8 matrix of known functions, known as the regressor. Equation (21) can be rewritten as

$$\dot{V} = \mathbf{s^T}[\mathbf{u_t} + \Psi(\mathbf{q}, \dot{\mathbf{q}}, t)\theta + \widetilde{\Delta}] \tag{23}$$

Noting the structure of (23), the following ARC law is proposed:

$$\mathbf{u_t} = \mathbf{u_a} + \mathbf{u_s};\ \mathbf{u_a} = -\Psi(\mathbf{q}, \dot{\mathbf{q}}, t)\widehat{\theta}; \tag{24}$$

where $\mathbf{u_a}$ is the adjustable model compensation needed for achieving perfect tracking, and $\mathbf{u_s}$ is a robust control law to be synthesized later. Substituting (24) into (23), and then simplifying the resulting expression lead to

$$\dot{V} = \mathbf{s^T}[\mathbf{u_s} - \Psi(\mathbf{q}, \dot{\mathbf{q}}, t)\widetilde{\theta} + \widetilde{\Delta}] \tag{25}$$

The robust control function $\mathbf{u_s}$ consists of two terms:

$$\mathbf{u_s} = \mathbf{u_{s1}} + \mathbf{u_{s2}},\ \mathbf{u_{s1}} = -\mathbf{Ks} \tag{26}$$

where $\mathbf{u_{s1}}$ is used to stabilize the nominal system, and it is a simple proportional feedback with $\mathbf{K}$ being a symmetric positive definite matrix in this case. And $\mathbf{u_{s2}}$ is a robust feedback used to attenuate the effect of model uncertainties. Noting Assumption 1 and (17) of (P4), there exists a $\mathbf{u_{s2}}$ such that the following two conditions are satisfied

$$\begin{aligned} i \quad & \mathbf{s^T}\{\mathbf{u_{s2}} - \Psi(\mathbf{q}, \dot{\mathbf{q}}, t)\widetilde{\theta} + \widetilde{\Delta}\} \leq \quad \eta \\ ii \quad & \mathbf{s^T u_{s2}} \leq \mathbf{0} \end{aligned} \tag{27}$$

where η is a design parameter that can be arbitrarily small. One smooth example of $\mathbf{u_{s2}}$ satisfying (27) is given by $\mathbf{u_{s2}} = -\frac{\mathbf{1}}{\mathbf{4}\eta}\mathbf{h^2 s}$, where $\mathbf{h}$ is a smooth function satisfying $\mathbf{h} \geq ||\theta_\mathbf{M}||||\Psi(\mathbf{q}, \dot{\mathbf{q}}, t)|| + \delta_\Delta$, and $\theta_M = \theta_{max} - \theta_{min}$.

Theorem 1: Suppose the adaptation function in (15) is chosen as

$$\tau = \Psi^\mathbf{T}(\mathbf{q}, \dot{\mathbf{q}}, t)\mathbf{s} \tag{28}$$

Then, the ARC control law (24) guarantees that:

A. In general, all signals are bounded. Furthermore, the positive semi-definite function $V(t)$ defined by (20) is bounded above by

$$V(t) \leq exp(-\lambda t)V(0) + \tfrac{\eta}{\lambda}[1 - exp(-\lambda t)] \tag{29}$$

where $\lambda = 2\sigma_{min}(\mathbf{K})/\mu_2$, and $\sigma_{min}(\cdot)$ denotes the minimum eigenvalue of a matrix. Note that $\sigma_{min}(\mathbf{K})$ is real and positive since $\mathbf{K}$ is symmetric positive definite.

B. Suppose there exist parametric uncertainties only after a finite time t_0, i.e., $\widetilde{\Delta} = 0$, $\forall t \geq t_0$. Then, in addition to result A, zero final tracking error is also achieved, i.e, $\mathbf{e} \to 0$ and $\mathbf{s} \to 0$ as $t \to \infty$.

V. Desired Compensation ARC (DCARC) Law

In the ARC design presented in section IV, the regressor $\Psi(\mathbf{q}, \dot{\mathbf{q}}, t)$ in the model compensation $\mathbf{u_a}$ (24) and the adaptation function τ (28) depend on states $\mathbf{q}$ and $\dot{\mathbf{q}}$. The idea of desired compensation ARC design in [12] was constructed to solve some implementation problems and complication of ARC. In the following, the desired compensation ARC is applied on the biaxial linear motor driven gantry.

The proposed DCARC law and adaptation function have the same form as (24) and (28), but with the regressor $\Psi(\mathbf{q}, \dot{\mathbf{q}}, t)$ substituted by the desired regressor $\Psi_\mathbf{d}(\mathbf{q_d}, \dot{\mathbf{q}}_\mathbf{d}, t)$:

$$\mathbf{u_t} = \mathbf{u_a} + \mathbf{u_s};\ \mathbf{u_a} = -\Psi_\mathbf{d}\widehat{\theta};\ \tau = \Psi_\mathbf{d}^\mathbf{T}\mathbf{s} \tag{30}$$

Choose a positive semi-definite function:

$$V(t) = \tfrac{1}{2}\mathbf{s}^\mathbf{T}\mathbf{M_t}\mathbf{s} + \tfrac{1}{2}\varepsilon^\mathbf{T}\mathbf{K}_\varepsilon\varepsilon \tag{31}$$

where $\mathbf{K}_\varepsilon$ is a s.p.d. matrix. Differentiating $V(t)$ and substituting (30) into the resulting expression yields

$$\dot{V} = \mathbf{s}^\mathbf{T}[\mathbf{u_s} + \widetilde{\Psi}\theta - \Psi_\mathbf{d}\widetilde{\theta} + \widetilde{\Delta}] + \varepsilon^\mathbf{T}\mathbf{K}_\varepsilon\dot{\varepsilon} \tag{32}$$

where $\widetilde{\Psi} = \Psi(\mathbf{q}, \dot{\mathbf{q}}) - \Psi_\mathbf{d}(\mathbf{q_d}, \dot{\mathbf{q}}_\mathbf{d})$ is the difference between the actual regression matrix and the desired regression matrix formulations. As shown in [13], $\widetilde{\Psi}$ can be quantified as

$$||\widetilde{\Psi}\theta|| \leq \zeta_1||\varepsilon|| + \zeta_2||\varepsilon||^2 + \zeta_3||\mathbf{s}|| + \zeta_4||\mathbf{s}||||\varepsilon|| \tag{33}$$

where $\zeta_1, \zeta_2, \zeta_3$ and ζ_4 are positive bounding constants that depend on the desired contour and the physical properties of the biaxial gantry. Similar to (26), the robust control function $\mathbf{u_s}$ consists of two terms given by:

$$\mathbf{u_s} = \mathbf{u_{s1}} + \mathbf{u_{s2}},\ \mathbf{u_{s1}} = -\mathbf{K}\mathbf{s} - \mathbf{K}_\varepsilon\varepsilon - \mathbf{K_a}||\varepsilon||^2\mathbf{s} \tag{34}$$

where the controller parameters $\mathbf{K}$, $\mathbf{K_e}$ and $\mathbf{K_a}$ are s.p.d. matrices satisfying $\sigma_{min}(\mathbf{K_a}) \geq \zeta_2 + \zeta_4$ and the following condition

$$\mathbf{Q} = \begin{bmatrix} \sigma_{min}(\mathbf{K}_\varepsilon\Lambda) - \frac{1}{4}\zeta_2 & -\frac{1}{2}\zeta_1 \\ -\frac{1}{2}\zeta_1 & \sigma_{min}(\mathbf{K}) - \zeta_3 - \frac{1}{4}\zeta_4 \end{bmatrix} > 0 \tag{35}$$

Specifically, it is easy to check that if

$$\sigma_{min}(\mathbf{K}_\varepsilon\Lambda) \geq \tfrac{1}{2}\zeta_1 + \tfrac{1}{4}\zeta_2, \sigma_{min}(\mathbf{K}) \geq \tfrac{1}{2}\zeta_1 + \zeta_3 + \tfrac{1}{4}\zeta_4 \tag{36}$$

the matrix $\mathbf{Q}$ defined in (35) is positive definite. The robust control term $\mathbf{u_{s2}}$ is required to satisfy the following constrains similar to (27),

$$\begin{aligned} i \quad & \mathbf{s}^\mathbf{T}\left\{\mathbf{u_{s2}} - \Psi_\mathbf{d}\widetilde{\theta} + \widetilde{\Delta}\right\} \leq \quad \eta \\ ii \quad & \mathbf{s}^\mathbf{T}\mathbf{u_{s2}} \leq \mathbf{0} \end{aligned} \tag{37}$$

One smooth example of $\mathbf{u_{s2}}$ satisfying (37) is $\mathbf{u_{s2}} = -\frac{1}{4\eta}h_d^2\mathbf{s}$, where h_d is any function satisfying $h_d \geq ||\theta_\mathbf{M}||||\Psi_\mathbf{d}|| + \delta_\triangle$.

Theorem 2: The desired compensation ARC law (30) guarantees that:

A. In general, all signals are bounded. Furthermore, the positive semi-definite function $V(t)$ defined by (31) is bounded above by

$$V(t) \leq exp(-\lambda t)V(0) + \tfrac{\eta}{\lambda}[1 - exp(-\lambda t)] \tag{38}$$

where $\lambda = \frac{2\sigma_{min}(\mathbf{Q})}{max[\mu_2, \sigma_{max}(\mathbf{K}_\varepsilon)]}$, and $\sigma_{max}(\cdot)$ denotes the minimum eigenvalue of a matrix.

B. Suppose there exist parametric uncertainties only after a finite time t_0, i.e., $\widetilde{\Delta} = 0$, $\forall t \geq t_0$. Then, in addition to result A, zero final tracking error is also achieved, i.e, $\varepsilon \to 0$ and $\mathbf{s} \to 0$ as $t \to \infty$.

VI. Experimental Setup and Results

A. Experiment setup

Figure 2. A Biaxial linear motor driven gantry system

To test the proposed controllers' effectiveness and study contour-following motion control of the biaxial gantry system, a biaxial Anorad gantry from Rockwell Automation is set up as a test-bed. As shown in Figure 2, the two axes of the gantry are mounted orthogonally with X-axis on top of Y-axis. The position sensors of the gantry are two linear encoders with a resolution of $0.5\mu m$ after quadrature. The velocity signal is obtained by the difference of two consecutive position measurements. Standard least-square identification is performed to obtain the parameters of the biaxial gantry and it is found that nominal values of the gantry system parameters without loads are $\theta = [0.12, 0.64, 0.166, 0.24, 0.1, 0.36, 0, 0]^T$. The bounds of the parametric variations are chosen as:

$$\begin{aligned} \theta_{min} &= [0.06, 0.5, 0.15, 0.1, 0.05, 0.08, -0.5, -1]^T \\ \theta_{max} &= [0.20, 0.75, 0.35, 0.3, 0.15, 0.5, 0.5, 1]^T \end{aligned} \tag{39}$$

B. Performance Index

The following performance indexes will be used to measure the quality of each control algorithm:

$\diamond$ $||\varepsilon_c||_{rms} = (\frac{1}{T}\int_0^T |\varepsilon_c|^2 dt)^{1/2}$, the rms value of the contouring error, is used to measure average contouring performance, where T represents the total running time;

$\diamond$ $\varepsilon_{cM} = \max_t\{|\varepsilon_c|\}$, the maximum absolute value of the contouring error is used to measure transient performance;

$\diamond$ $||u_i||_{rms} = (\frac{1}{T}\int_0^T |u_i|^2 dt)^{1/2}$, the average control input of each axis, is used to evaluate the amount of control effort.

C. Experimental Results

The control algorithms are implemented using a dSPACE DS1103 controller board. The controller executes programs at a sampling period $T_s = 0.2ms$, which results in a velocity measurement resolution of $0.0025m/sec$. The following control algorithms are compared:

C1: PID controllers for each axis separately. The control parameters are set as K_p, K_i, K_d. For X-axis, $K_p = 18000$, $K_i = 300000$, $K_d = 60$; for Y-axis, $K_p = 15000$, $K_i = 700000$, $K_d = 100$.

C2: ARC presented in section IV. The smooth functions $S_f(\dot{x})$ and $S_f(\dot{y})$ are chosen as $\frac{2}{\pi}arctan(9000\dot{x})$ and $\frac{2}{\pi}arctan(9000\dot{y})$. Λ is chosen as: $\Lambda = diag[100, 30]$. $\mathbf{u_{s2}}$ in (26) is theoretically given in section IV. In implementation, a large enough constant feedback gain is used instead to simplify the resulting control law as done in [14]. With this simplification, the feedback gain in (26) is chosen as: $\mathbf{K} = diag[100, 60]$ with ignoring $\mathbf{u_{s2}}$. The adaptation rates are set as $\Gamma = diag[10, 10, 10, 10, 1, 1, 10000, 10000]$. The initial parameter estimates are chosen as: $\widehat{\theta}(0) = [0.1, 0.55, 0.20, 0.22, 0.1, 0.15, 0, 0]^T$.

C3: DCARC presented in section V. The smooth functions $S_f(\dot{x}_d)$ and $S_f(\dot{y}_d)$ are chosen as $\frac{2}{\pi}arctan(9000\dot{x}_d)$ and $\frac{2}{\pi}arctan(9000\dot{y}_d)$. Λ is chosen as: $\Lambda = diag[100, 30]$. And the controller parameters in (34) are chosen as: $\mathbf{K} = diag[100, 60]$, $\mathbf{K_a} = diag[10000, 10000]$, and $\mathbf{K_e} = diag[5000, 5000]$. The adaptation rates are set as $\Gamma = diag[10, 10, 10, 10, 1, 1, 10000, 10000]$. For comparison purpose, the same initial conditions as those in ARC are used.

The following test sets are performed:

Set1 : To test the nominal contouring performance of the controllers, experiments are run without payload;

Set2 : To test the performance robustness of the algorithms to parameter variations, a 5 kg payload is mounted on the gantry;

Set3 : A large step disturbance (a simulated 0.6 V electrical signal) is added to the input of Y axis at t=1.86 sec and removed at t=4.86 sec to test the performance robustness of each controller to disturbance.

1) Circular contouring with constant velocity: The biaxial gantry is first commanded to track a circle given by

$$\mathbf{q_d} = \begin{bmatrix} x_d(t) \\ y_d(t) \end{bmatrix} = \begin{bmatrix} 0.2sin(2t) \\ -0.2cos(2t) + 0.2 \end{bmatrix} \quad (40)$$

which has a desired velocity of $v = 0.4m/sec$ on the contour.

2) Elliptical contouring with constant angular velocity: The gantry is also commanded to track an ellipse given by

$$\mathbf{q_d} = \begin{bmatrix} x_d(t) \\ y_d(t) \end{bmatrix} = \begin{bmatrix} 0.2sin(3t) \\ -0.1cos(3t) + 0.1 \end{bmatrix} \quad (41)$$

which has an angular velocity of $w = 3rad/sec$.

The experimental results of circular and elliptical contouring in terms of performance indexes after running the gantry for one period are given in Table I. Overall, both ARC and DCARC achieve good steady-state contouring performances which are quite better than those of PID. And as seen from the tables, DCARC performs better than ARC in terms of all the indexes. It also can be seen that ARC and DCARC controllers use almost the same amount of control efforts for every test set. Figure 3-5 show the circular contouring performances for the three sets. It's seen that both ARC and DCARC controllers achieve good contouring performances even in spite of the change of inertia load and uncertain disturbances. Figure 6-8 show the elliptical contouring performances which further illustrate that the proposed ARC and DCARC controllers achieve good contouring performances even there are parametric uncertainties and uncertain nonlinearities exist.

Circular contouring results				
	$\|\|\varepsilon_c\|\|_{rms}(\mu m)$	$\varepsilon_{cM}(\mu m)$	$\|\|u_x\|\|_{rms}(V)$	$\|\|u_y\|\|_{rms}(V)$
C1 (Set1)	4.06	18.02	0.23	0.44
C2 (Set1)	1.95	6.86	0.29	0.48
C3 (Set1)	1.77	6.33	0.30	0.50
C1 (Set2)	4.10	19.24	0.27	0.47
C2 (Set2)	2.13	8.55	0.30	0.51
C3 (Set2)	1.87	7.29	0.32	0.51
C1 (Set3)	4.51	41.84	0.24	0.44
C2 (Set3)	2.34	26.89	0.29	0.48
C3 (Set3)	2.06	23.28	0.30	0.49
Elliptical contouring results				
	$\|\|\varepsilon_c\|\|_{rms}(\mu m)$	$\varepsilon_{cM}(\mu m)$	$\|\|u_x\|\|_{rms}(V)$	$\|\|u_y\|\|_{rms}(V)$
C1 (Set1)	5.03	16.17	0.30	0.44
C2 (Set1)	2.67	9.55	0.36	0.49
C3 (Set1)	2.14	8.21	0.37	0.51
C1 (Set2)	5.29	17.90	0.36	0.48
C2 (Set2)	2.90	10.62	0.40	0.52
C3 (Set2)	2.35	9.31	0.40	0.53
C1 (Set3)	5.54	35.20	0.30	0.44
C2 (Set3)	3.07	24.56	0.36	0.49
C3 (Set3)	2.50	21.94	0.37	0.50

Table I
CONTOURING RESULTS

VII. CONCLUSIONS

This paper considers contour tracking controller design for a biaxial linear motor driven precision gantry in the presence of both parametric uncertainties and uncertain nonlinearities including unmodeled cogging forces and external disturbances. An ARC controller and a desired compensation ARC controller have been developed under the task coordinate framework formulation. The proposed controllers explicitly take into account the effect of model uncertainties coming from the inertia load, friction forces, and external disturbances. Extensive comparative experimental results for quite high speed both circular and elliptical motions have demonstrated the good contouring performance of the proposed ARC schemes in actual applications and the strong performance robustness to parameter variations and disturbances.

REFERENCES

[1] S. Komada, M. Ishida, K. Ohnishi, and T. Hori, "Disturbance observer-based motion control of direct drive motors," *IEEE Transactions on Energy Conversion*, vol. 6, no. 3, pp. 553–559, 1991.

[2] D. M. Alter and T. C. Tsao, "Control of linear motors for machine tool feed drives: design and implementation of h_∞ optimal feedback control," *ASME J. of Dynamic systems, Measurement, and Control*, vol. 118, pp. 649–656, 1996.

[3] L. Lu, Z. Chen, B. Yao, and Q. Wang, "Desired compensation adaptive robust control of a linear motor driven precision industrial gantry with improved cogging force compensation," *IEEE/ASME Transactions on Mechatronics*, vol. 13, no. 6, pp. 617–624, December 2008.
[4] G. T.-C. Chiu and M. Tomizuka, "Contouring control of machine tool feed drive systems: A task coordinate frame approach," *IEEE Trans. Control System Technology*, vol. 9, pp. 130–139, Jan. 2001.
[5] Y. Koren, "Cross-coupled biaxial computer control for manufacturing systems," *ASME J. Dynamical Systems, Measurement, and Control*, vol. 102, pp. 265–272, 1980.
[6] Y. Koren and C. C. Lo, "Variable gain cross coupling controller for contouring," *CIRP Proc.-Manuf. Syst.*, vol. 40, pp. 371–374, 1991.
[7] S.-S. Yeh and P.-L. Hsu, "Estimation of the contouring error vector for the cross-coupled control design," *IEEE/ASME Transactions on Mechatronics*, vol. 7, no. 1, March 2002.
[8] K.-H. Su and M.-Y. Cheng, "Contouring accuracy improvement using cross-coupled control and position error compensator," *Inter. J. of Machine Tools and Manufacture*, vol. 48, pp. 1444–1453, 2008.
[9] N. Chen, Y. Lou, and Z. Li, "Adaptive contouring control for high-accuracy tracking systems," in *IEEE International Conference on Systems, Man, and Cybernetics*, Taipei, Taiwan, October 2006.
[10] C.-L. Chen and K.-C. Lin, "Observer-based contouring controller design of a biaxial stage system subject to friction," *IEEE Transactions on Control System Technology*, vol. 16, no. 2, pp. 322–329, March 2008.
[11] B. Yao, "High performance adaptive robust control of nonlinear systems: a general framework and new schemes," in *IEEE Conference on Decision and Control*, 1997, pp. 2489–2494.
[12] ——, "Desired compensation adaptive robust control," in *The ASME International Mechanical Engineers Congress and Exposition (IMECE)*, vol. 64, 1998, pp. 569–575.
[13] N. Sadegh and R. Horowitz, "Stability and robustness analysis of a class of adaptive controllers for robot manipulators," *Int. J. Robotic Research*, vol. 9, no. 3, pp. 74–92, 1990.
[14] B. Yao, F. Bu, J. Reedy, and G. T.-C. Chiu, "Adaptive robust control of single-rod hydraulic actuators: theory and experiments," *IEEE/ASME Transactions on Mechatronics*, vol. 5, no. 1, pp. 79–91, 2000.

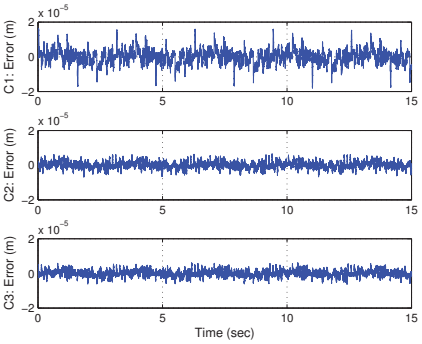

Figure 3. Circular contouring errors of Set1

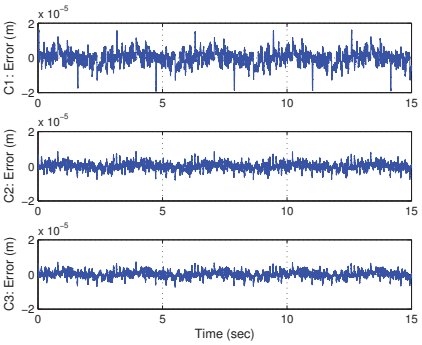

Figure 4. Circular contouring errors of Set2

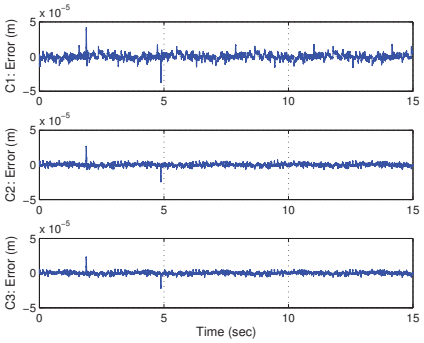

Figure 5. Circular contouring errors of Set3

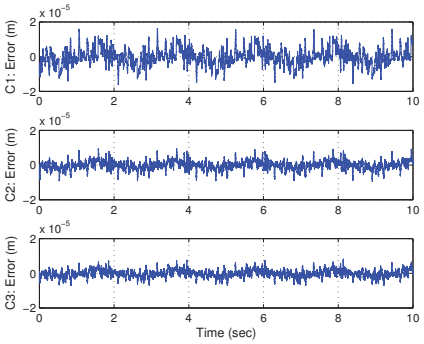

Figure 6. Elliptical contouring errors of Set1

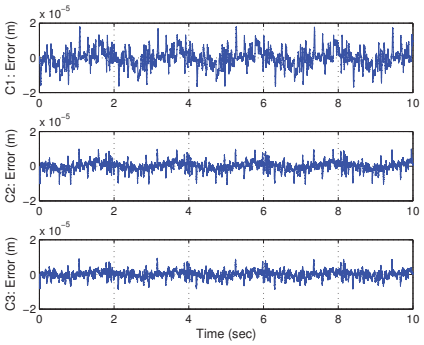

Figure 7. Elliptical contouring errors of Set2

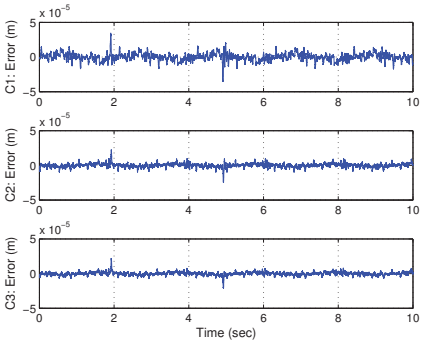

Figure 8. Elliptical contouring errors of Set3